Global analysis of aerosol properties above clouds

Waquet F., Peers P., Ducos F., Goloub P., Platnick S. E., Riedi J., Tanré D. and F. Thieuleux.

Abstract: The seasonal and spatial varability of Aerosol Above Cloud (AAC) properties are derived from passive satellite data for the year 2008. A significant amount of aerosols are transported above liquid water clouds on the global scale. For particles in the fine mode (i.e., radius smaller than 0.3 μm), including both clear sky and AAC retrievals increases the global mean aerosol optical thickness by 25 (±6) %. The two main regions with man-made AAC are the tropical Southeast Atlantic, for biomass burning aerosols, and the North Pacific, mainly for pollutants. Man-made AAC are also detected over the Arctic during the spring. Mineral dust particles are detected above clouds within the so-called "dust belt" region (5-40° N). AAC may cause a warming effect and bias the retrieval of the cloud properties. This study will then help to better quantify the impacts of aerosols on clouds and climate.

1. Introduction

Aerosols play a major role in the Earth's climate system through their interactions with solar radiation (direct effect), their influence on cloud properties (indirect and semi-direct effects) and the hydrological cycle [*Ramanathan et al.*, 2001]. Their negative forcing (cooling effect) may partially compensate for greenhouse gas effects. However, the radiative forcing due to both direct and indirect effects remains a large source of uncertainty. On the positive side, continuous global satellite observations provide reliable information about aerosol distributions and microphysical properties that can be used to improve radiative forcing estimates. Spatial measurements enable the distinction between natural and man-made aerosol signatures as long as they have different aerosols size distributions [*Tanré et al.*, 2001; *Kaufman*, 2005] and that some information on their geographical origin is available. The largest amount of natural aerosols is composed of mineral dust and sea salt, which mostly contribute to the coarse mode whereas man-made aerosols mainly come from urban and industrial pollution, and man-made vegetation fires which are dominated by fine mode particles (or accumulation mode) [*Kaufman et al.*, 2002]. Other aerosols mainly include volcanic dust, pollen and ash from wild vegetation fires.

Although elevated layers of aerosols are often transported above low-level clouds, most of aerosol property retrievals from global remote sensing observations are limited to cloud-free scenes. On a regional scale, several approaches have been developed to quantify the direct effect of aerosols above clouds (AAC) [e.g. *Hsu et al.*, 2003; *Chand et al.*, 2009; *Peters et al.*, 2011; *Meyer et al.*, 2013]. Overlying absorbing aerosols have an underestimated warming effect due to the reduction of the local planetary albedo. In addition to this direct effect, AAC such as biomass burning aerosols may influence the dynamical evolution of cloud that might lead to a cloud top altitude reduction and a cloud thickening [*Johnson et al.,* 2004; *Wilcox*, 2011]. Moreover, above cloud aerosols affect the retrieved values of the underlying cloud optical depth and effective radius [*Haywood et al.*, 2004; *Wilcox et al.*, 2009; *Coddington et al.*, 2010; *Meyer et al.*, 2013]. There is a lack of global observations about AAC loading and properties due to retrieval methods that are currently limited over space and time [*De Graaf et al.*, 2012; *Torres et al.*, 2012]. In spite of the ability of a satellite-borne lidar like CALIOP to detect aerosol and cloud vertical structure [*Chand et al.*, 2008; *Winker et al.*, 2012], the curtain observations have limited spatial coverage. Multidirectional polarization measurements have shown sensitivity to AAC scenes [*Waquet et al.*, 2009, 2012; *Hasekamp*, 2010; *Knobelspiesse et al.*, 2011]: aerosols generate an additional polarized light at side scattering angles and reduce the polarized signal of the cloud-bow. In light of these

observations and thanks to the A-Train, POLDER measurements combined with collocated and simultaneous information about clouds from MODIS paved the way for the development of a retrieval technique of AAC properties on a global scale for a year of data. These results, coupled with the clear-sky product over ocean (both fine and coarse mode) [*Herman et al.*, 2005] and over land (fine mode only) [*Deuzé et al.*, 2001] provided by POLDER are analyzed in this study.

2. Methodology

The operational algorithm proceeds as described by *Waquet et al.* [2013]. The "single pixel method" allows the retrieval of the Aerosol Optical Thickness (AOT) above liquid clouds and an aerosol model is chosen from the 7 models considesred by the algorithm (6 small spherical models for the fine mode and one non-spherical coarse model for dust). The method consists of a comparison between POLDER measurements at 670 and 865 nm and precomputed polarized radiances with a Successive Order of Scattering code [*Deuzé et al.*, 1989].

It should be noted that discrimination between fine mode aerosols and dust particles becomes inaccurate at small AOT. As a consequence, we first estimate AOT by only considering the six fine mode particles models and exclude the dust model if the AOT retrieved at the first step is smaller than 0.1 at 865 nm.

Several filters are then applied to enhance the quality of the product. Data that are not well-fitted to the models are rejected. Further, the variability of cloud properties within each POLDER pixel is evaluated from MODIS retrievals at higher resolution (1x1 km^2 at nadir) and only homogeneous pixels are kept [*Waquet et al.*, 2013]. The cloud optical thickness has to be larger than 3.0 to ensure the saturation of the polarized light scattered by the cloud layer. In order to avoid cirrus contamination, 3 additional criteria are added. The first one is based on the differences observed between the cloud top pressure provided by both MODIS (IR technique) and POLDER (Rayleigh and O_2 techniques). Secondly, the cloud phase index should not exceed 120, which corresponds to liquid clouds and "mixed-phase" clouds. The last criterion relies on a filter related to the Brightness Temperature Difference between the 8.6 and 11µm MODIS bands. This filter ($BTD_{8\text{-}11}$<-1.25K) is introduced since it has shown an ability to distinguish dust from cirrus [*Zhang et al.*, 2006; *Hansell et al.*, 2007].

Finally, data are aggregated from 6x6km^2 (POLDER native resolution at nadir) to 18x18km^2. We only keep the aggregated data for which the AOT standard deviation is smaller than 0.1 and that contain more than four 6x6km^2 POLDER pixels. This latter procedure allows to exclude cloud edges from the POLDER data.

3. Results

The study focuses on the analysis of global AOT (at 865 nm) and Ångström exponent retrieved over clouds during one year (see fig. 1, left and middle columns). We present average results for three month periods. The Ångström Exponent (AE) is computed using the mean AOT at 865 nm and 670 nm and it is only reported when the mean AOT is not equal to zero. The year is divided into four time periods: Winter (December 2007, January and February 2008, see fig 1, row 1); Spring (March, April and May 2008, row 2); Summer (June, July and August 2008, row 3) and Autumn (September, October and November 2008, row 4). The Ångström Exponent (AE) is computed using the mean AOT at 865 nm and 670 nm. Figure 1 also shows the number of retrievals (see right column).

The global features displayed in fig. 1 show that the properties of the AAC vary with season and location. AAC retrievals are mainly located over ocean and downwind of

continental sources. AAC retrievals with mineral dust particles are associated with the smallest values of AE. Fine mode AAC retrievals are associated with AOTs that mainly range between 0.1 and 0.2, knowing that fresh biomass-burning aerosols are related to AE larger than about 2.0. Values of AE of about 1 indicate regions influenced by both types of particles (i.e. mineral dust particles and fine mode particles).

Africa is the main contributor to biomass burning AAC retrievals. Man-made vegetation fires are frequently observed in Southern Africa between June and October and meteorological processes favor biomass burning aerosols transport to the west. During Summer, high mean AOT values (> 0.2) associated with small particles are retrieved over a large area located over the tropical southeast Atlantic region. Persistent low-level clouds are present over these regions during Summer. The AAC occurence is maximal for this season, with most retrievals detected off the coast of Angola (> 30). The mean AOT patterns over this region are consistent with the ones obtained from previous regional studies [e.g. *Chand et al.,* 2009]. Our results also reveal that the properties of biomass burning aerosols evolve during their transport above clouds. The mean AE progressively decreases from 2.5 to 1.7, from east to west (see fig. 2), which corresponds to an increase of 0.06 μm for the effective radius in our model database. This suggests that the mean size of the biomass burning aerosols increases as they progressively move away from the South African coast and age. The transport of African biomass burning aerosols above clouds over the Atlantic is also frequent during Autumn. A thick plume (AOT > 0.15) is observed crossing the South Atlantic, and almost reaching Brazil. The method also detects biomass burning AAC events over southeast Africa and the Indian Ocean, near the coasts of South Africa and southeastern Mozambique. These AAC occurences are observed in late August and increase in September and October, as the crop clearing fire season in Southern Africa progressively shifts from north to south. The AOT and AE maps also clearly show that biomass burning aerosols originating from southern Africa can be transported above clouds across the Indian Ocean over large distance as noted in earlier studies [e.g., *Swap et al.*, 2003; *Stein et al.*, 2003]. These biomass burning aerosols are transported east due to the prevailing wind in this region and reach Australia.

Asia is the second largest contributor of an-made AAC. Our results indicate that aerosol layers are transported above clouds across the North Pacific Ocean (35°N-60°N) from Asia to the USA. This transport occurs during the spring and summer seasons. Persistent thick low-level clouds cover this region and the number of AAC occurences are significant, especially during the Spring. Many fine mode particles were detected since several AAC with significant AOT (> 0.2) and AE of about 1.7 were observed, suggesting pollution aerosols (i.e. fine mode aerosols larger than biomass burning aerosols). Our results also indicate that mineral dust particles are transported across the North Pacific. For instance, mean AE of about 1.0 are retrieved near the coasts of Japan, during the Summer, and near the USA coast during the Spring. These results are consistent with previous studies showing transpacific asian aerosol pollution and mineral dust transport occurring during the spring and summer, with a peak in Spring [*Yu et al.,* 2008]. The pollution aerosols originate from the Asian megalopolis whereas the mineral dust particles originate from Mongolia and northeastern China deserts [*Prospero et al.,* 2002]. Fresh biomass burning aerosols (AE > 2.0) are also detected over the Okhotsk Sea, near the Siberian coast for the Spring and Summer. These aerosols are emitted by wild fires that frequently occur over eastern Siberia. Our results indicate that these biomass burning aerosols are also transported above clouds over the western North Pacific Ocean and are likely to contribute to the transpacific outflow.

The retrievals detect many AAC events associated with fine mode aerosols over the North Pole between mid-April and mid-June. The arctic haze phenomenon is seasonal (mainly spring) and has man-made origin [*Garrett and Verzella*, 2008], which is consistent with our results. Our daily result also exhibit large AE values (> 2.0) over this region, which

indicates that biomass burning aerosols are transported above clouds over the Arctic. Airbone measurements [*Quennehen et al.,* 2012] have shown that European air masses, with biomass burning aerosols, and Asian air masses, with contributions from both biomass burning aerosols and pollution particles (with soot-like inclusion), were transported to the pole during Spring 2008. Sometimes, the method also detected mineral dust AAC events over the Arctic in spring and our results indicate that various types of aerosols originated from eastern Asia (i.e. mineral dust and fine mode aerosols) contribute to the arctic haze.

AAC events associated with fine mode particles are also detected in other regions, including Autumn over North America, North Russia and near the west coast of Greenland. The method retrieves AE values of 1.7 for these AAC events, suggesting man-made aerosols. The nature of particles cannot be identified with confidence, since the AOT for these cases are generally small. The same type of AAC events were also detected over the North Atlantic, near the east coast of USA for the summer period. These aerosols may have originated from an industrial outflow from North America [*Coddington, et al.,* 2010]. Biomass burning AAC events are detected over a small area located over the south-east Asia (mainly over Vietnam and southern China) during the spring. These AAC events are related to man-made crop fires [*Hsu et al.,* 2003]. Some biomass burning AAC events were also detected along the coast of Califonia in June and July (see the AE maps for the Summer, AE > 2.0) that originated from local vegetation wild fires that occurred in California during the summer 2008. These events however do not result in a strong signal in our seasonal mean AOT.

Table 1 shows global mean results for AOT and the number of successful retrievals for the year 2008. We merged the aerosol products provided for the fine mode aerosols over ocean and land for clear-sky conditions with the ones retrieved above clouds. We computed a "all-sky" mean AOT that accounts for all successful retrievals performed for the three types of scenes. The method cannot identify with confidence the type of aerosols located above clouds for AOT smaller than 0.1. We then computed three estimates of this latter quantity by only considering fine mode AAC retrievals associated with (i) AOTs larger than 0.1, (ii) AOTs larger than 0.05 and (iii) by considering all fine mode AAC (see table 1). The comparison of the clear-sky and all-sky mean AOTs shows that accounting for AAC retrievals increases the global mean AOT for fine mode aerosols by 25 (±6) % for the year 2008.

The AE maps reveal four main regions with mineral dust above clouds: the tropical North East Atlantic region close to the Sahara, the Arabian sea, the southeastern part of the horn of Africa (mostly Ethiopia and Somalia) and the southeastern part of Asia. To a lesser extent, AAC events with mineral dust particles are also detected over northern Iran during the spring period and near the west coast of Australia during the boreal winter period. Mineral dust AAC is generaly associated with a small number of events and large mean values of AOT (see table 1). The transport of mineral dust particles above clouds is frequent over the south and east parts of Asia, throughout the year, with a maximum in spring. The other regions mainly show AAC events for the summer period. The transport of Saharan mineral dust is frequent across the Atlantic Ocean and mineral dust particles are often transported above low-level clouds near the coasts of North Africa [*Haywood et al.,* 2003]. Our methodology detects a large mineral dust plume extending over the tropical North East Atlantic between the African coast (12-14° in latitudes) and the middle of the Atlantic Ocean. The method retrieves mean AOT values between 0.3 and 0.9, with the maximal mean AOT retrieved near the coast of Mauritania. The main source areas for the Arabian Sea region could be the surrounding deserts located in Oman and in the Arabian Peninsula [*Prospero et al.,* 2002] whereas the mineral dust AAC observed over the horn of Africa could be originating from local sources previously detected in Ethiopia and Somalia [*Léon et al.,* 2003]. The analysis detects a dust plume over the middle of the North Atlantic Ocean during the winter period; AAC events with mineral dust particles are also detected along the northeastern coast

of the USA (AE of about 1.0) for the summer and spring periods and over the Gulf of Mexico for the spring period. We assume that these particles were transported from North Africa since the longe range transport of Saharan dust is frequent over the North Atlantic Ocean.

4. Conclusion

This study shows that the amount of man-made and natural aerosols transported above clouds is significant at the global scale. Current operational aerosol retrievals from passive sensors are restricted to cloud-free scenes and therefore significantly underestimate the total amount of aerosols. A positive above-cloud radiative forcing is typically expected when absorbing particles, such as biomass burning aerosols, are present above clouds though the magnitude (as well as the sign) depends on AOT, aerosol spectral single scattering albedo, and cloud optical thickness (e.g. *Keil and Haywood*, 2003). Our results indicate that a significant amount of such particles are transported above clouds in various regions of the world, including the North Pole during the Spring which was not expected. This suggests that the direct AAC forcing could be significant on a global scale. As previously mentioned, imager retrieved cloud property biases (primarily optical thickness and derived water path) are also expected when biomass burning aerosols and mineral dust particles are present above clouds and precautions should be therefore taken when analyzing cloud retrievals in regions where such AAC events are now identified. The fact that our method does not retrieve significant AOT over clouds in cloudy region located far away from continental sources, such as the Antarctic Ocean, is an encouraging sign. The use of a limited number of aerosol models and the lack of sensitivity to mineral dust particles, when the aerosol optical thicknesses above clouds becomes small, are two limitations, that could be overcome by using a more sophisticated retrieval method [e.g. *Waquet et al.,* 2013]. We also note that our method is currently restricted to AAC scenes with cloud optical thickness larger than 3.0 and homogenous liquid water clouds. The results presented in this study then probably underestimate the total number of AAC events. The above-cloud direct aerosol radiative effect increases with cloud optical thickness. We therefore identified in this study the AAC events that are the most important for estimating the radiative effect on a global scale.

Tables :

Results / Periods	Winter	Spring	Summer	Autumn	Total for

					2008
(a) Fine mode particles					
τ_{clear_sky}	0.026	0.027	0.026	0.027	0.026
τ_{all_sky} **($\tau_{cloud} \geq 0.00$)**	0.026	0.033	0.032	0.031	0.031
τ_{all_sky} **($\tau_{cloud} \geq 0.05$)**	0.030	0.036	0.039	0.035	0.034
τ_{all_sky} **($\tau_{cloud} \geq 0.10$)**	0.028	0.033	0.031	0.032	0.031
τ_{cloud} **($\tau_{cloud} \geq 0.00$)**	0.026	0.051	0.048	0.045	0.041
τ_{cloud} **($\tau_{cloud} \geq 0.05$)**	0.085	0.105	0.099	0.096	0.097
τ_{cloud} **($\tau_{cloud} \geq 0.10$)**	0.145	0.159	0.167	0.162	0.161
N_{clear_sky}	11039831	13546657	14249989	13587873	52611076
N_{cloud} **($\tau_{cloud} \geq 0.00$)**	5393916	4634317	5131051	5924123	21083407
N_{cloud} **($\tau_{cloud} \geq 0.05$)**	855146	1755204	1713771	1688658	6012779
N_{cloud} **($\tau_{cloud} \geq 0.10$)**	186726	633778	529621	489032	1839157
(b) Mineral dust particles					
τ_{cloud}	0.430	0.410	0.445	0.395	0.425
N_{cloud}	57746	132295	145217	64450	399708

Table 1. (a) Mean aerosol optical thickness and number of successful retrievals above clouds and clear-sky (ocean + land) scenes for the fine mode particles. N is the number of aerosol retrievals and τ is the aerosol optical thickness at 865 nm. The suffixes "cloud" and "clear_sky" refer to aerosol retrievals performed above clouds and over clear-sky scenes, respectively. The total optical thickness, τ_{all_sky}, is the mean aerosol optical thickness computed for all successfull retrievals performed for each type of scenes. (b) Mean aerosol optical thickness and number of aerosol retrievals estimated above clouds for mineral dust particles. The results shown in table 1 include AOT retrievals equal to 0.

Figures :

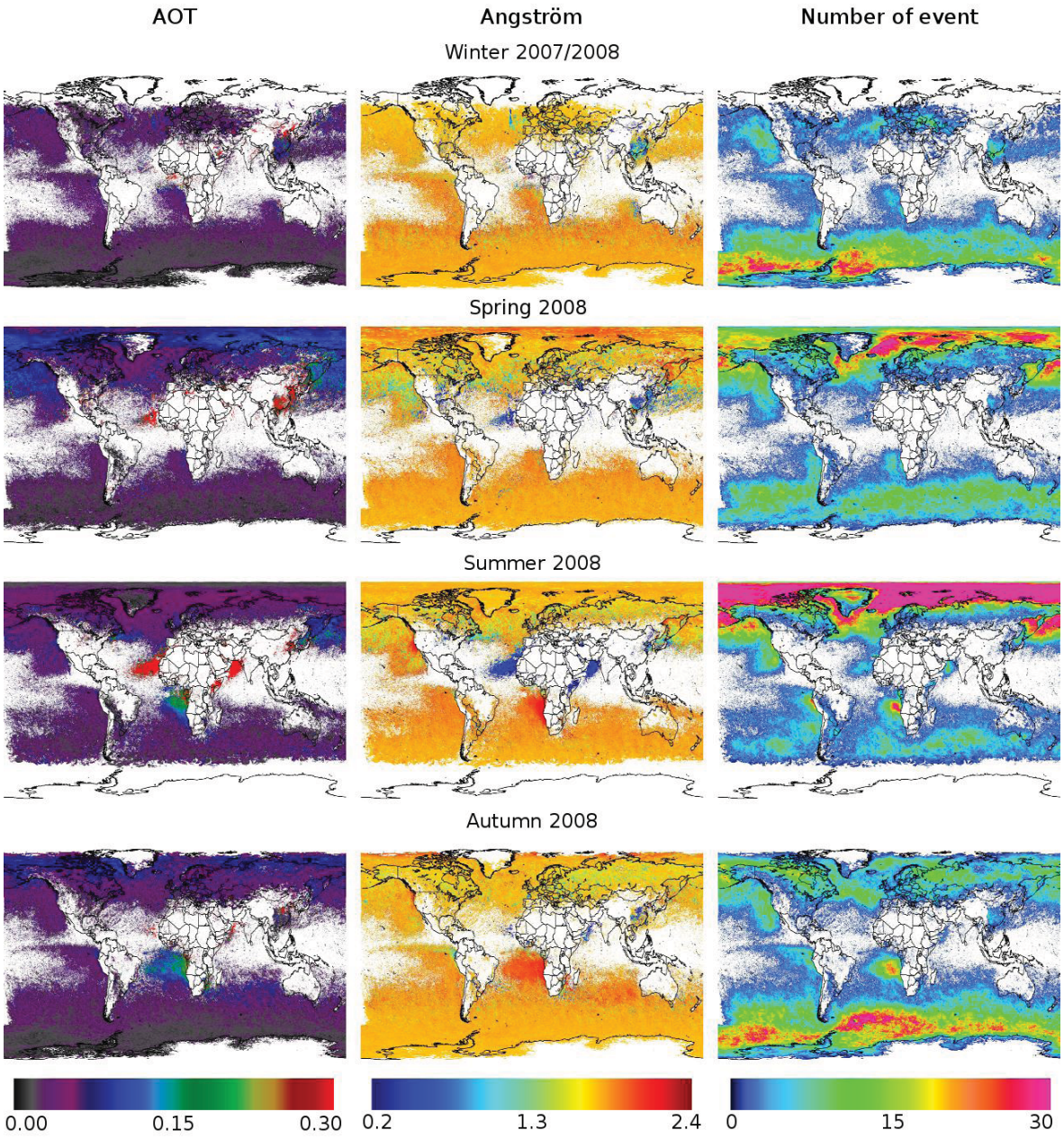

Figure 1. Global mean aerosol optical thickness at 865 nm (left column) and mean Ångström exponent (middle column) retrieved over clouds and number of retrievals (right column) in function of the season.

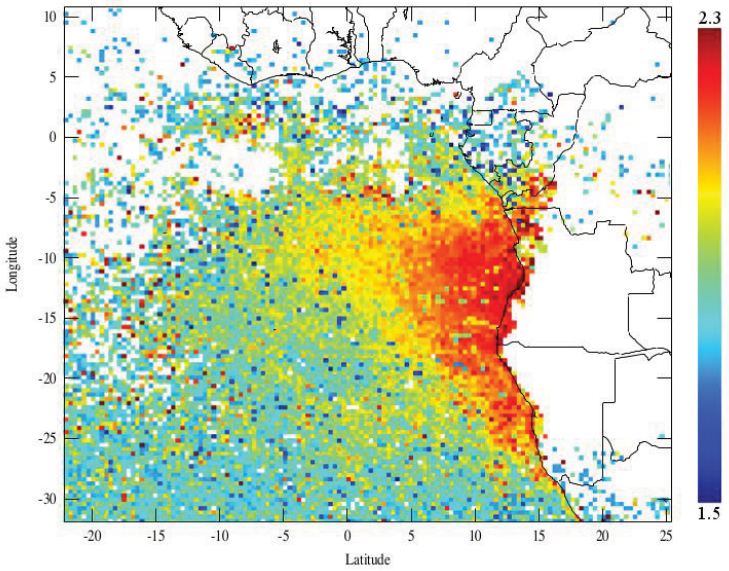

Figure 2. Ångström exponent retrieved above clouds by POLDER/PARASOL In the South Atlantic Ocean near South Africa. Mean values computed over 3 months (June, July and August 2008).

Acknowledgments :

This work has been supported by the Programme National de Télédétection Spatiale (PNTS, http://www.insu.cnrs.fr/actions-sur-projets/pnts-programme-national-de-teledetection spatiale), grant n° PNTS-2013-10. The authors are very grateful to CNES and NASA for providing the POLDER and MODIS data used in this study. We thank the ICARE data and services center for providing access to the data.

References :

Chand, D., T. L. Anderson, R. Wood, R. J. Charlson, Y. Hu, Z. Liu, and M. Vaughan (2008), Quantifying above-cloud aerosol using spaceborne lidar for improved understanding of cloudy-sky direct climate forcing, *Journal of Geophysical Research*, *113*(D13), 1–12, doi:10.1029/2007JD009433.

Chand, D., R. Wood, T. L. Anderson, S. K. Satheesh, and R. J. Charlson (2009), Satellite-derived direct radiative effect of aerosols dependent on cloud cover, *Nature Geoscience*, *2*(3), 181–184, doi:10.1038/ngeo437.

Coddington, O. M., P. Pilewskie, J. Redemann, S. Platnick, P. B. Russell, K. S. Schmidt, W. J. Gore, J. Livingston, G. Wind, and T. Vukicevic (2010), Examining the impact of overlying aerosols on the retrieval of cloud optical properties from passive remote sensing, *Journal of Geophysical Research*, *115*(D10), 1–13, doi:10.1029/2009JD012829.

Deuzé, J. L., M. Herman, and R. Santer (1989), Fourier series expansion of the transfer equation in the atmosphere-ocean system, *Journal of Quantitative Spectroscopy and Radiative Transfer*, *41*(6), 483–494, doi:10.1016/0022-4073(89)90118-0.

Deuzé, J. L., F. M. Bréon, C. Devaux, P. Goloub, M. Herman, B. Lafrance, F. Maignan, A. Marchand, F. Nadal, G. Perry, and D. Tanré (2001), Remote sensing of aerosols over land surfaces from POLDER-ADEOS-1 polarized measurements, *Journal of Geophysical Research*, *106*, 4913–4926, doi:10.1029/2000JD900364.

De Graaf, M., L. G. Tilstra, P. Wang, and P. Stammes (2012), Retrieval of the aerosol direct radiative effect over clouds from spaceborne spectrometry, *Journal of Geophysical Research*, *117*(D7), 1–18, doi:10.1029/2011JD017160.

Garrett and Verzella, an evolving history of artic aerosols (2008), BAMS, doi:10.1175/BAMS-89-3-299.

Hansell, R. A., S. C. Ou, K. N. Liou, J. K. Roskovensky, S. C. Tsay, C. Hsu, and Q. Ji (2007), Simultaneous detection/separation of mineral dust and cirrus clouds using MODIS thermal infrared window data, *Geophysical Research Letters*, *34*(11), 1–5, doi:10.1029/2007GL029388.

Hasekamp, O. P. (2010), Capability of multi-viewing-angle photo-polarimetric measurements for the simultaneous retrieval of aerosol and cloud properties, *Atmospheric Measurement Techniques Discussions*, *3*(2), 1229–1262, doi:10.5194/amtd-3-1229-2010.

Haywood, J. M., Osborne, S. R., Francis, P., Glew, M., Highwood, E., Formenti, P., and M. Andreae (2003), Radiative properties and direct radiative effect of Saharan dust measured by the C-130 aircraft during SHADE: 1. Solar spectrum, J. Geophys. Res., 108, 8577–8592, doi:10.1029/2002JD002687.

Haywood, J. M., S. R. Osborne, and S. J. Abel (2004), The effect of overlying absorbing aerosol layers on remote sensing retrievals of cloud effective radius and cloud optical depth, *Quarterly Journal of the Royal Meteorological Society*, *130*(598), 779–800, doi:10.1256/qj.03.100.

Herman, M. J-L. Deuzé, A. Marchand, B. Roger, and P. Lallart (2005), Aerosol remote sensing from POLDER/ADEOS over the ocean: Improved retrieval using a nonspherical particle model, *Journal of Geophysical Research*, *110*(D10), D10S02, doi:10.1029/2004JD004798.

Hsu, N. C., J. R. Herman, and S.-C. Chen (2003), Radiative impacts from biomass burning in the presence of clouds during boreal spring in southeast Asia, *Geophysical Research Letters*, *30*(5), 28–31, doi:10.1029/2002GL016485.

Johnson, B. T., K. P. Shine, and P. M. Forster (2004), The semi-direct aerosol effect: Impact of absorbing aerosols on marine stratocumulus. *Quarterly Journal of the Royal Meteorological Society*, *130*(599), 1407–1422. doi:10.1256/qj.03.61

Kaufman, Y. J., D. Tanré, and O. Boucher (2002), A satellite view of aerosols in the climate system., *Nature*, *419*(6903), 215–23, doi:10.1038/nature01091.

Kaufman, Y. J. O. Boucher, D. Tanré, M. Chin, L. A. Remer and T. Takemura (2005), Aerosol anthropogenic component estimated from satellite data, *Geophysical Research Letters*, *32*(17), 3–6, doi:10.1029/2005GL023125.

Keil, A. and Haywood, J. M.: Solar radiative forcing by biomass burning aerosol particles during SAFARI 2000: A case study based on measured aerosol and cloud properties, J. Geophys. Res., 108, 8467–8476, 2003.

Knobelspiesse, K., B. Cairns, J. Redemann, R. W. Bergstrom, and A. Stohl (2011), Simultaneous retrieval of aerosol and cloud properties during the MILAGRO field campaign, *Atmospheric Chemistry and Physics Discussions*, *11*(2), 6363–6413, doi:10.5194/acpd-11-6363-2011.

Léon, J.-F., and M. Legrand (2003), Mineral dust sources in the surroundings of the north Indian Ocean, Geophys. Res. Lett., 30(6), 1309, doi:10.1029/2002GL016690.

Meyer, K., S. Platnick, L. Oreopoulos, D. Lee (2013), Estimating the direct radiative forcing of absorbing aerosols overlying marine boundary layer clouds in the southeast Atlantic using MODIS and CALIOP. *J. Geophys. Res.*, 118, 4801-4815, DOI: 10.1002/jgrd.50449.

Nakajima, T., M. Tanaka, M. Yamano, M. Shiobara, K. Arao and Y. Nakanishi (1989), Aerosol optical characteristic in the yellow sand events observed in May, 1982 at

Nagasaki-Part 2 Models, J . Meteor. Soc. of Japan, 67, 279-291.

Peters, K., J. Quaas, and N. Bellouin (2011), Effects of absorbing aerosols in cloudy skies: a satellite study over the Atlantic Ocean, *Atmospheric Chemistry and Physics*, *11*(4), 1393–1404, doi:10.5194/acp-11-1393-2011.

Prospero, J. M., P. Ginoux, O. Torres, S. E. Nicholson, and T. E. Gill (2002), Environmental characterization of global sources of atmospheric soil dust identified with the nimbus 7 total ozone mapping spectrometer (TOMS) absorbing aerosol product, *Rev. Geophys.*, *40*(1), 1002, doi:10.1029/2000RG000095.

Quennehen, B., Schwarzenboeck, A., Matsuki, A., Burkhart, J. F., Stohl, A., Ancellet, G., and K. S. Law (2012): Anthropogenic and forest fire pollution aerosol transported to the Arctic: observations from the POLARCAT-France spring campaign, Atmos. Chem. Phys., 12, 6437-6454, doi:10.5194/acp-12-6437-2012.

Ramanathan, V., P. J. Crutzen, J. T. Kiehl, and D. Rosenfeld (2001), Aerosols, climate, and the hydrological cycle., *Science (New York, N.Y.)*, *294*(5549), 2119–24, doi:10.1126/science.1064034.

Stein, D. C., R. J. Swap, S. Greco, S. J. Piketh, S. A. Macko, B. G. Doddridge, T. Elias, and R. T. Bruintjes (2003), Haze layer characterization and associated meteorological controls along the eastern coastal region of southern Africa, J. Geophys. Res., 108(D13), doi:10.1029/ 2002JD003237.

Swap, R. J., H. J. Annegarn, J. T. Suttles, King, M. D., S. Platnick, J. L. Privette, and R. J. Scholes (2003), Africa burning: A thematic analysis of the Southern African Regional Science Initiative (SAFARI 2000). *J. Geophys. Res.*, 108, doi:10.1029/2003JD003747

Tanré, D., F. M. Bréon, J. L. Deuzé, M. Herman, P. Goloub, F. Nadal, and a. Marchand (2001), Global observation of anthropogenic aerosols from satellite, *Geophysical Research Letters*, *28*(24), 4555, doi:10.1029/2001GL013036.

Torres, O., H. Jethva, and P. K. Bhartia (2012), Retrieval of aerosol optical depth above clouds from OMI observations: Sensitivity analysis and case studies, *Journal of the Atmospheric Sciences*.

Waquet, F., Cornet, C., Deuzé, J.-L., Dubovik, O., Ducos, F., Goloub, P., Herman, M., Lapyonok, T., Labonnote, L. C., Riedi, J., Tanré, D., Thieuleux, F., and C. Vanbauce (2013), Retrieval of aerosol microphysical and optical properties above liquid clouds from POLDER/PARASOL polarization measurements, *Atmos. Meas. Tech.*, 6, 991-1016, doi:10.5194/amt-6-991-2013.

Wilcox, E. M., Harshvardhan, and S. Platnick (2009), Estimate of the impact of absorbing aerosol over cloud on the MODIS retrievals of cloud optical thickness and effective radius using two independent retrievals of liquid water path. *J. Geophys. Res.*, 114, doi:10.1029/2008JD010589.

Winker, D. M., J. L. Tackett, B. J. Getzewich, Z. Liu, M. A. Vaughan, and R. R. Rogers (2012), The global 3-D distribution of tropospheric aerosols as characterized by CALIOP. *Atmos. Chem. Phys. Discuss.*, 12, 24847–24893.

Yu, H., L. A. Remer, M. Chin, H. Bian, R. G. Kleidman, and T. Diehl (2008), A satellite-based assessment of transpacific transport of pollution aerosol, J. Geophys. Res., 113, D14S12, doi:10.1029/2007JD009349.

Zhang, P., N. Lu, X. Hu, and C. Dong (2006), Identification and physical retrieval of dust storm using three MODIS thermal IR channels, *Global and Planetary Change*, *52*(1-4), 197–206, doi:10.1016/j.gloplacha.2006.02.014.